

Measurement of $B \rightarrow D^{*-}\tau^+\nu_\tau$ and $B \rightarrow h^{(*)}\nu\bar{\nu}$ Decays at Belle

K.-F. Chen

Department of Physics, National Taiwan University, Taipei

We report an observation of the decay $B^0 \rightarrow D^{*-}\tau^+\nu_\tau$ and a search for the rare decays $B \rightarrow h^{(*)}\nu\bar{\nu}$, where $h^{(*)}$ stands for a light meson. A data sample of 535 million $B\bar{B}$ pairs collected with the Belle detector at the KEKB e^+e^- collider is used. We find a signal with a significance of 5.2 standard deviations on $B^0 \rightarrow D^{*-}\tau^+\nu_\tau$ and measure the branching fraction to be $2.02^{+0.40}_{-0.37}(\text{stat.}) \pm 0.37(\text{syst.})\%$. No significant signal is observed for $B \rightarrow h^{(*)}\nu\bar{\nu}$ decays and we set upper limits on the branching fractions at 90% confidence level. The limits on $B^0 \rightarrow K^{*0}\nu\bar{\nu}$ and $B^+ \rightarrow K^+\nu\bar{\nu}$ decays are more stringent than the previous constraints, while the first searches for $B^0 \rightarrow K^0\nu\bar{\nu}$, $\pi^0\nu\bar{\nu}$, $\rho^0\nu\bar{\nu}$, $\phi\nu\bar{\nu}$ and $B^+ \rightarrow K^{*+}\nu\bar{\nu}$, $\rho^+\nu\bar{\nu}$ are presented.

1. Introduction

The decay $B^0 \rightarrow D^{*-}\tau^+\nu_\tau$ is dominated by the $b \rightarrow c$ transition and can provide the important information associated with the charge Higgs in the Standard Model (SM). The τ lepton in the final state provide additional observables sensitive to the physics beyond SM, as well as the τ polarization, which cannot be accessed in other semileptonic decays. However, the neutrinos in the final states and the low efficiencies from τ reconstruction make the search to be very challenging. The SM predict a $B \rightarrow \bar{D}^*\tau^+\nu_\tau$ branching fraction of 1.4% [2], while there are several experimental results provided by the LEP experiments; the averaged $b \rightarrow \tau\nu_\tau X$ semi-inclusive branching fraction is $2.48 \pm 0.26\%$ [1].

The flavor-changing neutral-current process $B \rightarrow h^{(*)}\nu\bar{\nu}$ is sensitive to physics beyond the SM. The SM branching fractions are estimated to be 1.3×10^{-5} and 4×10^{-6} for $B \rightarrow K^*\nu\bar{\nu}$ and $B \rightarrow K\nu\bar{\nu}$ decays [3], respectively, and are expected to be much lower for other modes. Theoretical calculation of the decay amplitudes for these decays is particularly reliable, because of the absence of long-distance interactions that affect charged-lepton channels $B \rightarrow h^{(*)}l^+l^-$. New physics such as SUSY particles or a possible fourth generation could potentially contribute to the penguin loop or box diagram and enhance the amplitudes [3]. Reference [4] also discusses the possibility of discovering light dark matter in $b \rightarrow s$ transitions with large missing momentum. Due to the challenge of cleanly detecting rare modes with two final-state neutrinos, only a few studies of $h^{(*)}\nu\bar{\nu}$ have been carried out to date [5, 6, 7].

In this report, we present the first observation of the decay $B^0 \rightarrow D^{*-}\tau^+\nu_\tau$ and the search for the decays $B \rightarrow h^{(*)}\nu\bar{\nu}$ ($h^{(*)}$ stands for K^+ , K_S^0 , K^{*0} , K^{*+} , π^+ , π^0 , ρ^0 , ρ^+ , and ϕ) using a 492 fb^{-1} data sample recorded at the $\Upsilon(4S)$ resonance, corresponding to 535×10^6 B -meson pairs. Throughout this report, the inclusion of charge conjugate decays is implied unless otherwise stated. The Belle detector is a large-solid-angle magnetic spectrometer located at the KEKB collider [8], and is described in detail elsewhere [9].

2. $B^0 \rightarrow D^{*-}\tau^+\nu_\tau$

We select charged tracks that are associated with the interaction point (IP). The electrons candidates are selected using the information from particle identification systems. The four momenta of electron candidates are corrected for bremsstrahlung radiation by adding photons within a 50 mrad cone along the track direction. The π^0 candidates are reconstructed from pairs of photon with the invariant mass in the range 118 MeV/ c^2 and 150 MeV/ c^2 . Minimum energies of 60–120 MeV are required for the photon candidates from π^0 decays, according to different polar angles. Photons that are not included in $p\pi^0$ reconstruction and exceed a polar-angle dependent energy threshold (100–200 MeV) are included in the tag-side B -meson (B_{tag}) reconstruction.

Reconstruction of the B_{tag} strongly suppresses the combinatorial and continuum backgrounds and provides kinematical constraints on the signal meson (B_{sig}). We take the advantage of the clean signature, supported by the D^* meson at the signal side. The B_{tag} meson is reconstructed using all the particles that remain after selecting candidates for B_{sig} decay daughters. The D^* mesons are reconstructed through the following decay chain: $D^{*+} \rightarrow D^0\pi^+$, $D^0 \rightarrow K^-\pi^+$ and $K^-\pi^+\pi^0$. The τ leptons are reconstructed in $\tau \rightarrow e^+\nu_e\bar{\nu}_\tau$ and $\pi^+\bar{\nu}_\tau$ decays, while the $\tau \rightarrow \mu^+\nu_e\bar{\nu}_\tau$ mode is excluded due to the inefficient muon identification in the relevant momentum range. For $\tau^+ \rightarrow \pi^+\bar{\nu}_\tau$ decays, only $D^0 \rightarrow K^-\pi^+$ mode is used in order to avoid the higher combinatorial background.

Once a D^{*+} candidate is reconstructed and a charged track expected from τ^+ is selected, the remaining particles measured by the detector are used to reconstruct the B_{tag} . Two kinematical variables, $M_{\text{tag}} = \sqrt{E_{\text{beam}}^2 - p_{\text{tag}}^2}$ and $\Delta E_{\text{tag}} = E_{\text{tag}} - E_{\text{beam}}$, are used to identify the B_{tag} candidates, where E_{beam} is the beam energy. The momentum (p_{tag}) and energy (E_{tag}) of the B_{tag} meson is calculated by a summation over all particles that are not assigned to B_{sig} . The signal candidates are required to satisfy

$M_{\text{tag}} > 5.2 \text{ GeV}/c^2$ and $|\Delta E_{\text{tag}}| < 0.6 \text{ GeV}$ at least. To improve the purity of the selected B_{tag} candidates, several additional requirements are imposed, such as zero total event charge, no additional leptons in the event, zero baryon number. The residual energy in the ECL should be smaller than 0.35 GeV and number of neutral particles (π^0 and γ) included for the tag side should be less than 5. The B_{tag} reconstruction algorithm is verified using the control sample, $B_{\text{sig}} \rightarrow D^{*-}\pi^+$, and is found to be consistent with Monte Carlo (MC) simulations.

The dominated background source is from the semileptonic $B \rightarrow D^*e\nu_e$ decays for $\tau^+ \rightarrow e^+\nu_e\bar{\nu}_\tau$ mode, and combinatorial background from hadronic B decays for $\tau^+ \rightarrow \pi^+\bar{\nu}_\tau$ decays. Further background suppression is achieved with the following variables: the missing energy $E_{\text{mis}} = E_{\text{beam}} - E_{D^*} - E_{e,\pi}$, visible energy of the event, the square of missing mass $M_{\text{mis}}^2 = E_{\text{mis}}^2 - (p_{\text{sig}} - p_{D^*} - p_{e,\pi})^2$, and the effective mass of $\tau\nu_\tau$ system $M_W^2 = (E_{\text{beam}} - E_{D^*})^2 - (p_{\text{sig}} - p_{D^*})^2$. The most effective variable X_{mis} is defined by $(E_{\text{mis}} - |p_{D^*} + p_{e,\pi}|) / \sqrt{E_{\text{beam}}^2 - m_{B^0}^2}$, which is closely related to the missing mass but does not depend on B_{tag} reconstruction.

We extract the signal yields by maximum likelihood fits to the M_{tag} distributions. The likelihood function is given by

$$\mathcal{L} = e^{-(N_s + N_p + N_b)} \prod_{i=1}^N [(N_s + N_p)P_s(M_{\text{tag}}^i) + N_bP_b(M_{\text{tag}}^i)], \quad (1)$$

where P_s (P_b) is the probability density function (PDF) for signal and combinatorial background events, and N_s , N_p , and N_b denote the yields for signal, peaking background, and combinatorial background, respectively. The signal distribution is described using a Crystal Ball lineshape function [10], and the background part is parameterized using the ARGUS-function [11]. The number of N_s and N_b are float parameters in the fit, while the N_p is fixed to the value obtained from MC simulation, and fixed to zero for $\tau^+ \rightarrow \pi^+\bar{\nu}_\tau$ decays. The fit results are included in Table I, and the distributions of M_{tag} and ΔE_{tag} from data with fit results superimposed are shown in Figure 1. The combined branching fraction is $2.02^{+0.40}_{-0.37}\%$, and is obtained using a fit with a constraint to a common value.

The systematic uncertainties include the number of B -meson pairs (1.3%), signal shape (2.8%), parameterization of the combinatorial background (5.7%) which is estimated by varying the ARGUS-shape parameters. An 8.2% uncertainty is included for the peaking background, which is dominated by MC statistics. The uncertainty in B_{tag} reconstruction (10.9%) is evaluated from the control sample. Efficiency uncertainties in the tracking, neutral reconstruction and particle identification are in the range

Table I Summary of signal yield (N_s), reconstruction efficiencies (ϵ), branching fraction (\mathcal{B}), and statistical significance (Σ) for $B \rightarrow D^{*-}\tau^+\nu_\tau$ decays.

| subchannel | N_s | $\epsilon(10^{-4})$ | $\mathcal{B}(\%)$ | Σ |
|--|-----------------------|---------------------|------------------------|----------|
| $D^0 \rightarrow K^-\pi^+$, $\tau^+ \rightarrow e^+\nu_e\bar{\nu}_\tau$ | $19.5^{+5.8}_{-5.0}$ | 3.25 | $2.44^{+0.74}_{-0.65}$ | 5.0 |
| $D^0 \rightarrow K^-\pi^+\pi^0$, $\tau^+ \rightarrow e^+\nu_e\bar{\nu}_\tau$ | $11.9^{+6.0}_{-5.2}$ | 0.78 | $1.69^{+0.84}_{-0.74}$ | 2.6 |
| $D^0 \rightarrow K^-\pi^+$, $\tau^+ \rightarrow \pi^+\bar{\nu}_\tau$ | $29.9^{+10.0}_{-9.1}$ | 1.07 | $2.02^{+0.68}_{-0.61}$ | 3.8 |
| Combined | 60^{+12}_{-11} | 1.17 | $2.02^{+0.40}_{-0.37}$ | 6.7 |

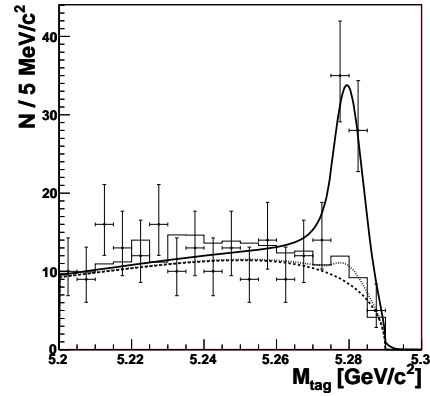


Figure 1: M_{tag} and ΔE_{tag} distributions for $B \rightarrow D^{*-}\tau^+\nu_\tau$ candidates from data. The solid curve shows the fit results, and the dot-dashed curves indicate the background component. The open-histograms shows the background distributions from MC simulations.

of 7.9–10.7%, according to different decay channels. The uncertainties due to the partial sub ratios are taken from PDG [1]. The combined uncertainty is 18.5%, and the statistical significance signal is reduced to 5.2σ including the systematic uncertainties.

In conclusion, we observe 60^{+12}_{-11} events for the decay $B^0 \rightarrow D^{*-}\tau^+\nu_\tau$ based on a data sample of 535×10^6 $B\bar{B}$ pairs. This is the first observation of an exclusive B decays with $b \rightarrow c\tau\bar{\nu}_\tau$ transition. The measured branching fraction $2.02^{+0.40}_{-0.37} \pm 0.37\%$ is consistent with the prediction in SM.

3. $B \rightarrow h^{(*)}\nu\bar{\nu}$

The decays $B \rightarrow h^{(*)}\nu\bar{\nu}$ are reconstructed in a different way. Candidate $e^+e^- \rightarrow \Upsilon(4S) \rightarrow B\bar{B}$ events are characterized by a fully-reconstructed B_{tag} . The B_{tag} candidates are reconstructed in one of the following modes: $B^0 \rightarrow D^{(*)-}\pi^+$, $D^{(*)-}\rho^+$, $D^{(*)-}a_1^+$, $D^{(*)-}D_s^{(*)+}$, $B^+ \rightarrow \bar{D}^{(*)0}\pi^+$, $\bar{D}^{(*)0}\rho^+$,

$\overline{D}^{(*)0}a_1^+$, and $\overline{D}^{(*)0}D_s^{(*)+}$. The D^- mesons are reconstructed as $D^- \rightarrow K_S^0\pi^-, K_S^0\pi^-\pi^0, K_S^0\pi^-\pi^+\pi^-, K^+\pi^-\pi^-,$ and $K^+\pi^-\pi^-\pi^0$. The following decay channels are included for \overline{D}^0 mesons: $\overline{D}^0 \rightarrow K^+\pi^-, K^+\pi^-\pi^0, K^+\pi^-\pi^+\pi^-, K_S^0\pi^0, K_S^0\pi^-\pi^+, K_S^0\pi^-\pi^+\pi^0$ and K^-K^+ . The D^{*-} (\overline{D}^{*0}) mesons are reconstructed as $\overline{D}^0\pi^-$ ($\overline{D}^0\pi^0$ and $\overline{D}^0\gamma$). Furthermore, $D_s^{*+} \rightarrow D_s^+\gamma, D_s^+ \rightarrow K_S^0K^+$ and $K^+K^-\pi^+$ decays are reconstructed. B_{tag} candidates are selected using the beam-energy constrained mass $M_{\text{bc}} \equiv \sqrt{E_{\text{beam}}^2 - p_B^2}$ and the energy difference $\Delta E \equiv E_B - E_{\text{beam}}$. We require B_{tag} candidates satisfy the requirements $M_{\text{bc}} > 5.27 \text{ GeV}/c^2$ and $-80 \text{ MeV} < \Delta E < 60 \text{ MeV}$. We reconstruct 7.88×10^5 and 4.91×10^5 charged and neutral B mesons, respectively.

The rest of particles in the event are used to reconstruct a $B_{\text{sig}} \rightarrow h^{(*)}\nu\overline{\nu}$ candidate. Prompt charged tracks are required to associated with IP, and a minimum momentum of 0.1 GeV/ c in the transverse plane. We select kaon and pion from charged tracks based on the particle identification system. Pairs of oppositely charged tracks are used to reconstruct $K_S^0 \rightarrow \pi^+\pi^-$ decays. For $\pi^0 \rightarrow \gamma\gamma$, a minimum photon energy of 50 MeV is required and the $\gamma\gamma$ invariant mass must be within $\pm 16 \text{ MeV}/c^2$ of the nominal π^0 mass.

The decays $B_{\text{sig}} \rightarrow K^+\nu\overline{\nu}, \pi^+\nu\overline{\nu}, K_S^0\nu\overline{\nu}$, and $\pi^0\nu\overline{\nu}$ are reconstructed from single K^+, π^+, K_S^0 , and π^0 candidates, respectively. The $B^0 \rightarrow K^{*0}\nu\overline{\nu}$ candidate is reconstructed from a charged pion and an oppositely charged kaon, while $B^+ \rightarrow K^{*+}\nu\overline{\nu}$ decays are reconstructed from a K_S^0 candidate and a charged pion, or a charged kaon and a π^0 candidate. The reconstructed mass of the K^{*0} (K^{*+}) candidate should be within a $\pm 75 \text{ MeV}/c^2$ window around the nominal K^{*0} (K^{*+}) mass. Furthermore, pairs of charged pions with opposite charge are used to form $B^0 \rightarrow \rho^0\nu\overline{\nu}$ candidates where the $\pi^+\pi^-$ invariant mass should be within $\pm 150 \text{ MeV}/c^2$ from the nominal ρ^0 mass. For $B^+ \rightarrow \rho^+\nu\overline{\nu}$, a charged pion and a π^0 candidate are used, and a $\pm 150 \text{ MeV}/c^2$ mass window is required. A ϕ meson is formed from a K^+K^- pair with a reconstructed mass within $\pm 10 \text{ MeV}/c^2$ from the nominal ϕ mass.

We reject the events with additional charged tracks or π^0 candidates, and select B_{sig} candidates using the variable $E_{\text{ECL}} \equiv E_{\text{tot}} - E_{\text{rec}}$, where E_{tot} and E_{rec} are the total visible energy measured by the ECL detector and the measured energy of reconstructed objects including the B_{tag} and the signal side $h^{(*)}$ candidate, respectively. The decays $B \rightarrow D^*\ell\nu$ are examined as control samples; the observed E_{ECL} distributions are found to be in good agreement with MC simulations. The signal region is defined by $E_{\text{ECL}} < 0.3 \text{ GeV}$ while the sideband region is given by $0.45 \text{ GeV} < E_{\text{ECL}} < 1.5 \text{ GeV}$.

The dominant background source is $B\overline{B}$ decays involving a $b \rightarrow c$ transition. A lower bound of 1.6 GeV/ c on P^* , the momentum of the $h^{(*)}$ (except ϕ) in the B_{sig} rest frame, suppresses this background, while

an upper bound of 2.5 GeV/ c rejects the contributions from radiative two-body modes such as $B \rightarrow K^*\gamma$. The cosine of the angle between the missing momentum in the laboratory frame and the beam is required to lie between -0.86 and 0.95 . Other background sources are found to be small.

The data E_{ECL} distributions are shown in Figure 2. The distributions of background are estimated with MC simulations and are normalized by the number of events in the sideband region. None of the signal modes has a significant signal. Including the effects of both statistical and systematic uncertainties, an extension of the Feldman-Cousins method [12, 13] is used to calculate the upper limits. The observed number of events in the signal box and sideband region, expected background contributions in the signal box, reconstruction efficiencies, and the obtained upper limits at 90% confidence level (CL) are shown in Table II. The reconstruction efficiencies are estimated with MC simulations using the $B \rightarrow h^{(*)}$ form factors from Ref. [14]. The $B^0 \rightarrow \phi\nu\overline{\nu}$ MC samples are generated with the $B \rightarrow K^*$ form factors.

Table II A summary of the number of observed events in the signal box (N_{obs}), expected background yields (N_b) in the signal box, reconstruction efficiencies including both B_{tag} and B_{sig} (ϵ), and the upper limits (U.L.) at 90% CL.

| Mode | N_{obs} | N_b | $\epsilon(\times 10^{-5})$ | U.L. |
|---------------------------|------------------|----------------|----------------------------|------------------------|
| $K^{*0}\nu\overline{\nu}$ | 7 | 4.2 ± 1.4 | 5.1 ± 0.3 | $< 3.4 \times 10^{-4}$ |
| $K^{*+}\nu\overline{\nu}$ | 4 | 5.6 ± 1.8 | 5.8 ± 0.7 | $< 1.4 \times 10^{-4}$ |
| $\rightarrow K_S^0\pi^+$ | 1 | 2.3 ± 1.2 | 2.8 ± 0.3 | |
| $\rightarrow K^+\pi^0$ | 3 | 3.3 ± 1.4 | 3.0 ± 0.4 | |
| $K^+\nu\overline{\nu}$ | 10 | 20.0 ± 4.0 | 26.7 ± 2.9 | $< 1.4 \times 10^{-5}$ |
| $K^0\nu\overline{\nu}$ | 2 | 2.0 ± 0.9 | 5.0 ± 0.3 | $< 1.6 \times 10^{-4}$ |
| $\pi^+\nu\overline{\nu}$ | 33 | 25.9 ± 3.9 | 24.2 ± 2.6 | $< 1.7 \times 10^{-4}$ |
| $\pi^0\nu\overline{\nu}$ | 11 | 3.8 ± 1.3 | 12.8 ± 0.8 | $< 2.2 \times 10^{-4}$ |
| $\rho^0\nu\overline{\nu}$ | 21 | 11.5 ± 2.3 | 8.4 ± 0.5 | $< 4.4 \times 10^{-4}$ |
| $\rho^+\nu\overline{\nu}$ | 15 | 17.8 ± 3.2 | 8.5 ± 1.1 | $< 1.5 \times 10^{-4}$ |
| $\phi\nu\overline{\nu}$ | 1 | 1.9 ± 0.9 | 9.6 ± 1.4 | $< 5.8 \times 10^{-5}$ |

The possible disagreement in the E_{ECL} distributions between data and MC is checked using wrong-flavor combinatorial events, and an uncertainty of 0.1–2.0 events is included. Background contributions from rare B decays are examined using a large MC sample and the variation in the background yield (0.1–1.8 events) is included as a systematic uncertainty. The uncertainties in B_{tag} reconstruction (2.0% for B^0 and 9.9% for B^\pm) are estimated by comparing the yields of data and MC from the B_{tag} candidates. Systematic uncertainty arising from the track and π^0 rejection is studied using $B \rightarrow D^{(*)}\ell\nu$ decays, and an error of 2.7% is assigned. The uncertainties in the efficiencies including detecting a K_S^0 (4.9%) or π^0

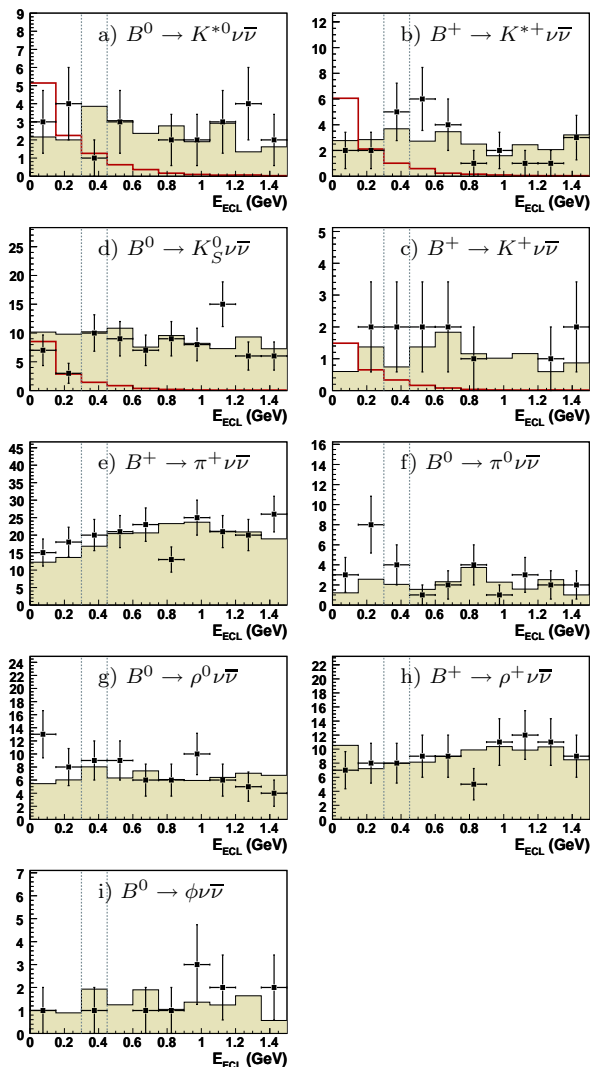


Figure 2: The E_{ECL} distributions for $B \rightarrow h^{(*)} \nu \bar{\nu}$ decays. The shaded histograms show the background distributions from MC simulations and are normalized to sideband data. The open histograms show the SM expected signal distributions for $B \rightarrow K^{(*)} \nu \bar{\nu}$ decays multiplied by a factor of 20 for the comparison. The vertical dashed lines show the upper bound (left) of the signal box and the lower bound (right) of the sideband region.

(4.0%), $B \rightarrow h^{(*)}$ form factors (0.4–13%), the number of $B\bar{B}$ events (1.3%), tracking efficiency (1.0–2.2%), particle identification (0.5–2.0%), $h^{(*)}$ mass selection (0.8–2.3%), and the $\phi \rightarrow K^+ K^-$ branching fraction (1.2%).

We have performed a search for $B \rightarrow h^{(*)} \nu \bar{\nu}$ decays with a fully reconstructed B tagging method on a data sample of 535×10^6 $B\bar{B}$ pairs. No significant signal is observed and we set upper limits on the branching fractions at 90% CL. The limits obtained for $B^0 \rightarrow K^{*0} \nu \bar{\nu}$ and $B^+ \rightarrow K^+ \nu \bar{\nu}$ decays are more stringent than the previous constraints. The first searches for

$B^0 \rightarrow K^0 \nu \bar{\nu}$, $\pi^0 \nu \bar{\nu}$, $\rho^0 \nu \bar{\nu}$, $\phi \nu \bar{\nu}$, and $B^+ \rightarrow K^{*+} \nu \bar{\nu}$, $\rho^+ \nu \bar{\nu}$ are carried out. The results still allow room for substantial non-SM contributions, thus a higher luminosity B -factory experiment is required to probe the SM predictions for the branching fractions.

Acknowledgments

We thank the KEKB group for excellent operation of the accelerator, the KEK cryogenics group for efficient solenoid operations, and the KEK computer group and the NII for valuable computing and SuperSINET network support. We acknowledge support from MEXT and JSPS (Japan); ARC and DEST (Australia); NSFC and KIP of CAS (China); DST (India); MOEHRD, KOSEF, KRF and SBS Foundation (Korea); KBN (Poland); MES and RFAAE (Russia); ARRS (Slovenia); SNSF (Switzerland); NSC and MOE (Taiwan); and DOE (USA).

References

- [1] W.-M. Yao *et al.* (Particle Data Group), J. Phys. G **33**, 1 (2006).
- [2] J. G. Körner and G. A. Schuler, Phys. Lett. B **231**, 306 (1989); D. S. Hwang and D. W. Kim, Eur. Phys. J. C **14**, 271 (2000); C.-H. Chen and C.-Q. Geng, Phys. Rev. D **71**, 077501 (2005).
- [3] G. Buchalla, G. Hiller and G. Isidori, Phys. Rev. D **63**, 014015 (2000).
- [4] C. Bird, P. Jackson, R. Kowalewski and M. Pospelov, Phys. Rev. Lett. **93**, 201803 (2004).
- [5] W. Adam *et al.* (DELPHI Collaboration), Z. Phys. C **72**, 207 (1996).
- [6] T. E. Browder *et al.* (CLEO Collaboration), Phys. Rev. Lett. **86**, 2950 (2001).
- [7] B. Aubert *et al.* (BaBar Collaboration), Phys. Rev. Lett. **94**, 101801 (2005).
- [8] S. Kurokawa and E. Kikutani, Nucl. Instrum. Methods Phys. Res., Sect. A **499**, 1 (2003).
- [9] A. Abashian *et al.* (Belle Collaboration), Nucl. Instrum. Methods Phys. Res., Sect. A **479**, 117 (2002).
- [10] T. Skwarnicki, Ph.D. Thesis, Institute of Nuclear Physics, Krakow 1986; DESY Internal Report, DESY F31-86-02 (1986).
- [11] H. Albrecht *et al.* (ARGUS Collaboration), Phys. Lett. B **241**, 278 (1990).
- [12] G. J. Feldman and R. D. Cousins, Phys. Rev. D **57**, 3873 (1998).
- [13] J. Conrad, O. Botner, A. Hallgren and C. Perez de los Heros, Phys. Rev. D **67**, 012002 (2003).
- [14] P. Ball and R. Zwicky, Phys. Rev. D **71**, 014015 (2005); Phys. Rev. D **71**, 014029 (2005).